

## **Supporting Information**

# **Achieving Type I, II, and III Heterojunctions Using Functionalized MXene**

Youngbin Lee, Yubin Hwang, and Yong-Chae Chung\*

Department of Materials Science and Engineering, Hanyang University

Seoul, 133-791, Republic of Korea

\*E-mail: [yongchae@hanyang.ac.kr](mailto:yongchae@hanyang.ac.kr), tel: +82-2-2220-0507

### Band structure of three monolayer components with the HSE06 functional

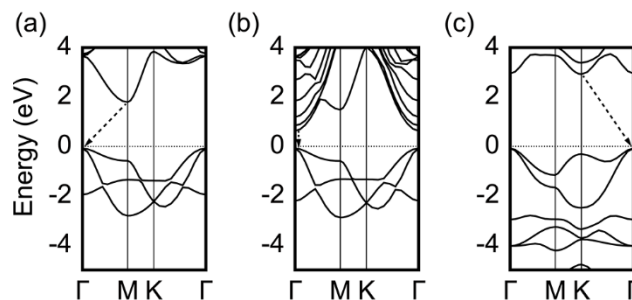


**Figure S1.** Band structure of the functionalized monolayer  $\text{Sc}_2\text{C}$  with the HSE06 functional. The band structure of monolayer (a)  $\text{Sc}_2\text{CF}_2$ , (b)  $\text{Sc}_2\text{C}(\text{OH})_2$ , and (c)  $\text{Sc}_2\text{CO}_2$ . The Fermi level was set to zero, and the arrows indicate the recombination pathways for the excitons in each monolayer.

The band structures were calculated using the HSE06 functional (Figure S1). From the results, it is obtained that the band gaps of monolayer  $\text{Sc}_2\text{CF}_2$ ,  $\text{Sc}_2\text{C}(\text{OH})_2$ , and  $\text{Sc}_2\text{CO}_2$  are increased to 1.88, 0.71, and 3.01 eV, respectively. However, when the band structures of all systems are compared with the results from the PBE functional, shapes of the band structures are preserved and positions of the conduction band minimum (CBM) and valence band maximum (VBM) are exactly same. Thus, it can be concluded that the calculation using the PBE functional will give reliable results about the heterojunction type of the functionalized  $\text{Sc}_2\text{C}$  bilayer heterosystems.

## Modeling of the functionalized $\text{Sc}_2\text{C}$ heterostructure

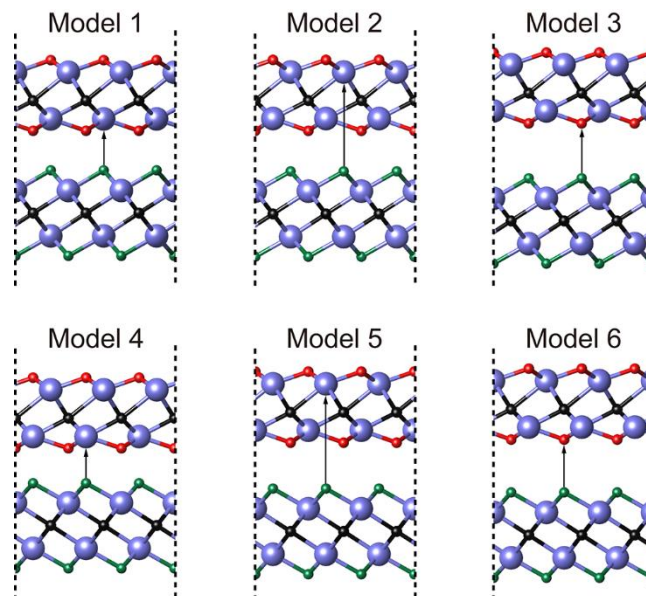


**Figure S2.** Possible high symmetry stacking patterns for modeling each functionalized  $\text{Sc}_2\text{C}$  heterostructure. The arrow indicates the atom that the functional atom of the bottom layer directly points to. The F/O (A) system is presented as a representative functionalized  $\text{Sc}_2\text{C}$  heterosystem.

Among the geometries of the  $\text{Sc}_2\text{CX}_2/\text{Sc}_2\text{CY}_2$  ( $\text{X}/\text{Y}$ ,  $\text{X}$  and  $\text{Y} = \text{F}, \text{OH}, \text{O}$ ) heterostructures using three functionalized monolayer  $\text{Sc}_2\text{C}$ , six high symmetry models were considered regarding each interface type (F/OH, O/OH (A), O/OH (B), F/O (A), F/O (B)), as shown in Figure S2. Here, the notations (A) and (B) in the O/OH and F/O heterostructures represent the heterosystems with an interface including the  $\text{O}_\text{A}$  and  $\text{O}_\text{B}$  sides of the monolayer  $\text{Sc}_2\text{CO}_2$ , respectively. Each pattern was sorted into an arrangement of the bottom layer and the type of the atom directly indicated by the functional atom of the bottom layer. Each optimized

heterosystem was determined as the structure with the lowest total energy among the six models by a strict energy convergence test. The most stable configurations were Model 3, 6, 3, 4, and 1 at the F/OH, O/OH (A), O/OH (B), F/O (A), and F/O (B) systems, respectively (Figure S2).

### Change of the energy gaps in the F/OH and O/OH heterosystems by the biaxial strain

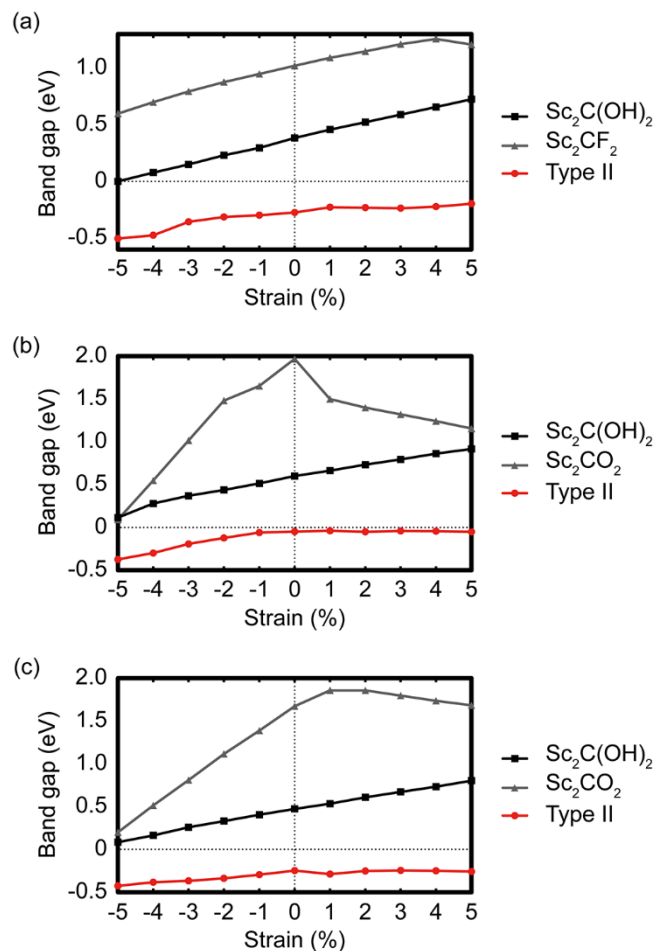


**Figure S3.** Change in the energy gaps between the CBM and the VBM levels of the total heterostructure systems and each single-layer in the systems as a function of the strain: (a) F/OH, (b) O/OH (A), and (c) O/OH (B) systems. The black, gray, and red lines represent the energy gap of the Sc<sub>2</sub>C(OH)<sub>2</sub>, Sc<sub>2</sub>CF<sub>2</sub> (Sc<sub>2</sub>CO<sub>2</sub>), and type-II heterostructure, respectively. The energy gap of the type-II heterostructure was obtained from the difference between the CBM state of Sc<sub>2</sub>CF<sub>2</sub> (Sc<sub>2</sub>CO<sub>2</sub>) and the VBM state of Sc<sub>2</sub>C(OH)<sub>2</sub> in the F/OH (O/OH) system.

To confirm a heterojunction type transition in the F/OH and O/OH heterostructures by an

equibiaxial strain, the changes in each energy gap in the systems as a function of the strain are presented in Figure S3. In the three heterosystems, the energy gaps of the type-II heterostructure are preserved as negative values under all strains. Therefore, it is known that the F/OH and O/OH heterostructures maintain a type-III heterojunction despite the strain effect.

## Bonding character of the functionalized Sc<sub>2</sub>C heterostructures

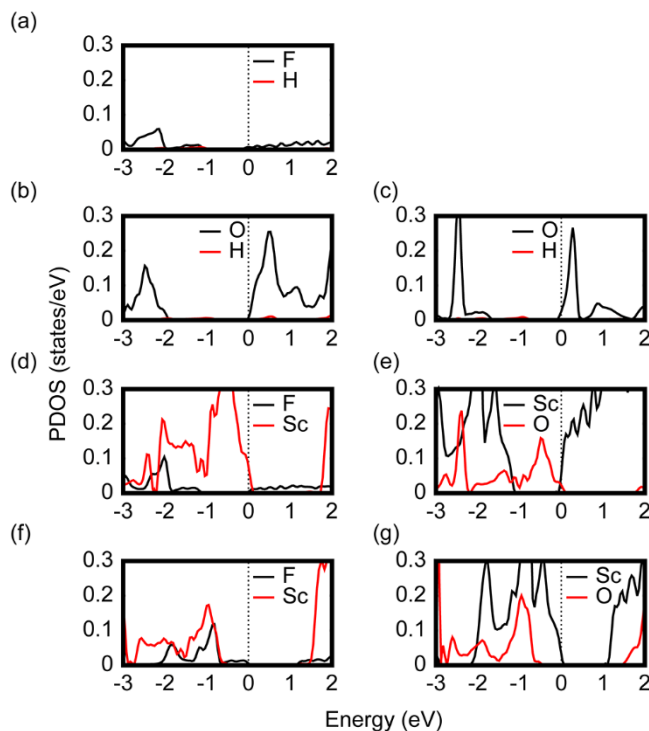


**Figure S4.** PDOS of the nearest atoms at the interface in the (a) F/OH, (b) O/OH (A), (c) O/OH (B), (d)-(e) F/O (A), and (f)-(g) F/O (B) heterostructures. In the two F/O systems, the two PDOS are presented due to the two interlayer bonds between the functional group of each layer and the Sc atom of the opposite layer. The black and red lines indicate each nearest atom to the opposite layers.

To verify factors retaining the heterojunction in the functionalized Sc<sub>2</sub>C heterosystems, adhesive energies with and without the van der Waals correction were calculated (Table S1). The values with the van der Waals correction signify the adhesive energies including effects of both chemical and physical interactions, and these values were calculated using the DFT-D2 method. On the other hand, the values without the van der Waals correction from the

calculation with the pure PBE functional imply the adhesive energies originating from only chemical interaction. From these results, it can be concluded that chemical reaction as well as physical interaction have an effect on the functionalized Sc<sub>2</sub>C heterostructures.

To clarify how the chemical reaction influences on the functionalized Sc<sub>2</sub>C heterostructures, the interlayer charge transfer and the partial density of states (PDOS) of the nearest atoms between each monolayer are shown in Figure 5 and S4, respectively. The charge transfer occurs at the interface in all the bilayer heterostructures (Figure 5). In particular, the values are relatively large in the F/OH and O/OH (B) systems whose adhesive energies are mainly affected by the chemical reaction. On the other hand, it was found that the heterojunctions in the functionalized Sc<sub>2</sub>C heterostructures are little related to covalent bonding because there is no hybridization between the nearest atoms in the interface (Figure S4). Thus, these results show that the chemical reaction primarily originates from the charge transfer between two monolayer components.

**Table S1.** Adhesive energies with and without the van der Waals correction of the most stable configuration for each X/Y heterostructure.

$E_{ad}$ [meV/Å <sup>2</sup> ]	F/OH	O/OH (A)	O/OH (B)	F/O (A)	F/O (B)
With correction	36	17	46	31	36
Without correction	24	4	31	6	10



### Plane-averaged electrostatic potential of three monolayer components

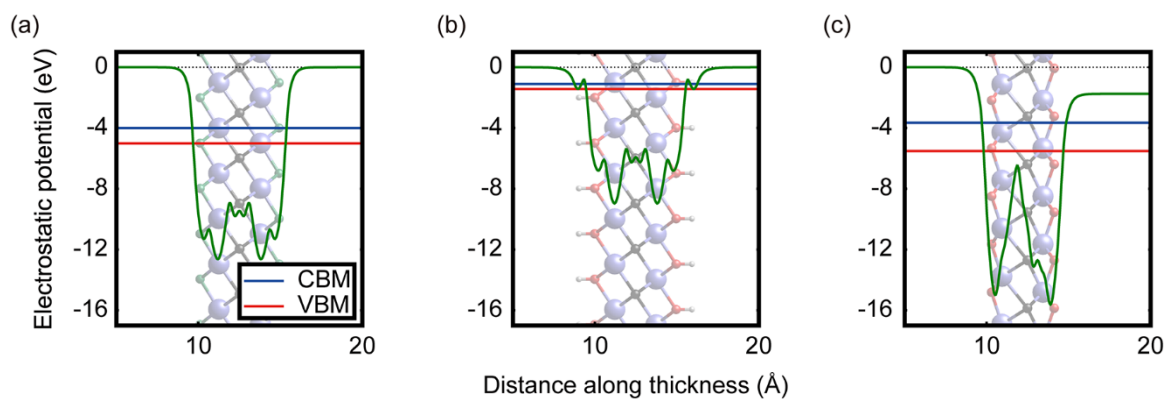


**Figure S5.** Plane-averaged electrostatic potential along the thickness direction of the monolayer (a)  $\text{Sc}_2\text{CF}_2$ , (b)  $\text{Sc}_2\text{C}(\text{OH})_2$ , and (c)  $\text{Sc}_2\text{CO}_2$ . The vacuum level at the bottom surface was set to zero, and the CBM and VBM states are presented as the blue and red horizontal lines, respectively. The positions of the atoms in each monolayer are indicated by the background.

### Estimated band alignment of the F/O (B) system related to the HSE06 functional

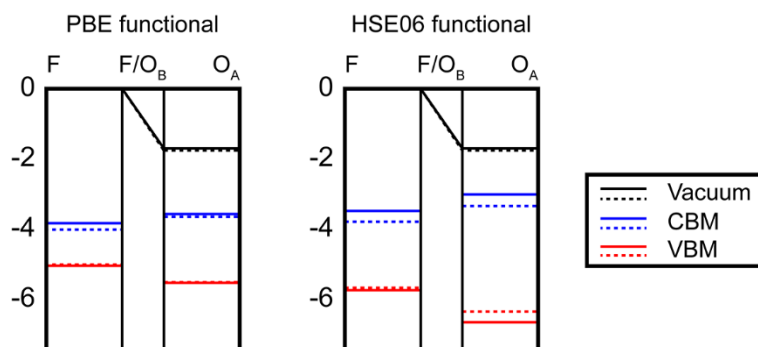


**Figure S6.** Band alignment of each component in the F/O (B) system before and after the heterojunction using the PBE and HSE06 functionals. The dashed and solid lines represent the band alignment before and after the heterojunction, respectively. The black, blue, and red lines indicate the vacuum level at surface of the F/O (B) heterosystem, and the CBM and VBM levels in each monolayer, respectively. A higher vacuum level of both surfaces was set to zero. The vacuum level at the other surface of the F/O (B) heterostructure and the CBM and VBM levels in each monolayer are presented relative to zero. Because the vacuum levels of components are same in the interface of the heterostructure, the vacuum level in the interface was not included.

From a previous work, it was reported that the band-edge position related to the HSE06 functional can be supposed from the result of the PBE functional in semiconductor and insulator.<sup>1</sup> Here, the band alignment related to the HSE06 functional was estimated in the F/O (B) system, which is only semiconductor among the functionalized Sc<sub>2</sub>C heterostructures. The band gaps of three functionalized monolayer Sc<sub>2</sub>C systems from the HSE06 functional are 1.86 times larger than those with the PBE functional on average (Figure 1 and S1). To estimate the band gap of the F/O (B) system when the HSE06 functional is used, each gap of

components in the heterosystem was multiplied by 1.86.<sup>1</sup> Then, the CBM (VBM) was briefly shifted upwards (downwards) by  $1/3\Delta E_g$  ( $2/3\Delta E_g$ ,  $\Delta E_g = E_{g[\text{HSE}]} - E_{g[\text{PBE}]}$ ,  $E_{g[\text{HSE}]}$  and  $E_{g[\text{PBE}]}$ : the band gap using the HSE06 and PBE functionals, respectively) from the result with the PBE functional.<sup>1</sup> From these results, the estimated HSE06 band alignment was obtained (Figure S6). Although this process does not give the exact band alignment, it has a significant meaning to give a more reasonable idea about the properties of the calculated band gap.

## REFERENCES

- (1) Chen, W.; Pasquarello, A. Band-Edge Levels in Semiconductors and Insulators: Hybrid Density Functional Theory versus Many-Body Perturbation Theory. *Phys. Rev. B* **2012**, 86, 035134.